The American Journal of Pathology, Vol. 173, No. 5, November 2008

DOI: 10.2353/ajpath.2008.071153

Vascular Biology, Atherosclerosis and Endothelium Biology

Involvement of the Lysophosphatidic Acid-Generating Enzyme Autotaxin in Lymphocyte-Endothelial Cell Interactions

Tae Nakasaki,*† Toshiyuki Tanaka,* Shinichi Okudaira,§ Michi Hirosawa,* Eiji Umemoto,* Kazuhiro Otani,* Soojung Jin,* Zhongbin Bai,* Haruko Hayasaka,* Yoshinori Fukui,¶ Katsuyuki Aozasa,§ Naoya Fujita,‖ Takashi Tsuruo,‖ Keiichi Ozono,† Junken Aoki,§ and Masayuki Miyasaka*

From the Department of Microbiology and Immunology, Laboratory of Immunodynamics, the Department of Developmental Medicine (Pediatrics),† and the Department of Pathology,‡ Osaka University Graduate School of Medicine, Osaka; the Department of Molecular and Cellular Biochemistry,§ Graduate School of Pharmaceutical Sciences, Tohoku University, Miyagi; the Division of Immunogenetics,¶ Department of Immunobiology and Neuroscience, Medical Institute of Bioregulation, Kyushu University, Fukuoka; and the Cancer Chemotherapy Center,‖ Japanese Foundation for Cancer Research, Tokyo, Japan*

Autotaxin (ATX) is a secreted protein with lysophospholipase D activity that generates lysophosphatidic acid (LPA) from lysophosphatidylcholine. Here we report that functional ATX is selectively expressed in high endothelial venules (HEVs) of both lymph nodes and Peyer's patches. ATX expression was developmentally regulated and coincided with lymphocyte recruitment to the lymph nodes. In adults, ATX expression was independent of HEV-expressed chemokines such as CCL21 and CXCL13, innate immunity signals including those via TLR4 or MyD88, and of the extent of lymphocyte trafficking across the HEVs. ATX expression was induced in venules at sites of chronic inflammation. Receptors for the ATX enzyme product LPA were constitutively expressed in HEV endothelial cells (ECs). *In vitro*, LPA induced strong morphological changes in HEV ECs. Forced ATX expression caused cultured ECs to respond to lysophosphatidylcholine, up-regulating lymphocyte binding to the ECs in a LPA receptor-dependent manner under both static and flow conditions. Although *in vivo* depletion of circulating ATX did not affect lymphocyte trafficking into the lymph nodes, we surmise, based on the above data, that ATX expressed by HEVs acts on HEVs *in situ* to facilitate lymphocyte binding to ECs and that ATX in the general circulation does not play a major role in this process. Tissue-specific inactivation of ATX will verify this hypothesis in future studies of its mechanism of action. ***(Am J Pathol 2008, 173:1566–1576; DOI: 10.2353/ajpath.2008.071153)***

Much of the efficiency of the immune system depends on continual lymphocyte recirculation through the secondary lymphoid tissues. Lymphocyte recirculation begins with blood lymphocytes interacting with the endothelial wall of high endothelial venules (HEVs) in lymph nodes (LNs) and Peyer's patches (PPs), in a process called lymphocyte rolling. The rolling brings lymphocytes into contact with HEV endothelial cells (ECs), which express a variety of chemokines and adhesion molecules. Lymphocytes bind to these molecules and transmigrate through the HEVs.[1,2] This interaction between lymphocytes and the molecules on HEV ECs is transient and reversible, and both lymphocytes and HEV ECs show marked and coordinated morphological changes during the process,[3] indicating that each of the two cell types acts on the other. The molecular details behind these interactions, however, remain to be fully elucidated.

Accumulating evidence indicates that a variety of lysophospholipids act on immune cells by transmitting signals through a family of G-protein-coupled receptors to control the cells' differentiation, motility, and survival.[4] In

Supported in part by the Ministry of Education, Culture, Sports, Science, and Technology of Japan (grants-in-aid 17047025 to T.T., 17046010 to T.T., 17590432 to T.T., and 17014056 to M.M.).

N.T. and T.T. contributed equally to this study.

Accepted for publication July 18, 2008.

Present address of T.T.: Laboratory of Immunobiology, School of Pharmacy, Hyogo University of Health Sciences, Kobe, Japan.

Address reprint requests to Dr. Masayuki Miyasaka, Laboratory of Immunodynamics, Department of Microbiology and Immunology, Osaka University Graduate School of Medicine, 2-2, Yamada-oka, Suita, Osaka, 565-0871, Japan. E-mail: mmiyasak@orgctl.med.osaka-u.ac.jp.

particular, structurally related lysophospholipid mediators such as sphingosine-1-phosphate (S1P) and lysophosphatidic acid (LPA), which can be generated from lipid stores by cellular enzymatic pathways in macrophages, dendritic cells, mast cells, and platelets, act on lymphocytes and dendritic cells through members of the S1P-receptor family ($S1P_1 \sim S1P_5$) and the LPA-receptor family ($LPA_1 \sim LPA_5$), respectively.[4–7] Among these ligand-receptor interactions, S1P and its receptor $S1P_1$ are required for thymocyte emigration[8] as well as lymphocyte egress from the secondary lymphoid tissues,[9,10] although exactly where and how these signaling molecules function is not fully understood. In addition, the functional significance of the interaction between LPA and its receptors in the immune system is unknown.

Autotaxin (ATX), originally identified as a tumor motility-stimulating protein,[11] is a secreted protein identical to lysophospholipase D (lysoPLD).[12] *In vitro*, ATX converts lysophosphatidylcholine (LPC) and sphingosylphosphorylcholine to LPA[12] and S1P,[13] respectively. However, a recent study indicates that ATX is a major producer of LPA, but not of S1P, *in vivo*.[14] Under physiological conditions, ATX is expressed in the central nervous system and is implicated in oligodendrocyte function.[15] In addition, ATX transcripts have been found in human tonsillar HEVs,[16] but its protein expression has not been reported in HEVs, let alone its function. While this manuscript was under review, Kanda and colleagues[17] published that ATX is involved in lymphocyte trafficking from blood into lymphoid tissues.

Here we report that ATX is preferentially expressed in the HEVs of mouse LNs and PPs and that its expression correlates positively with the ability of venules to support lymphocyte trafficking across the endothelial walls. ATX was clearly inducible in chronically inflamed venules that mediate pathological lymphocyte trafficking. Interestingly, LPA receptors were expressed in HEV ECs, and the addition of LPA caused substantial cytoskeletal changes. Forced ATX expression made cultured ECs reactive to LPC, which up-regulated lymphocyte binding to the ECs in a LPA receptor-dependent manner. Because ATX is a major producer of LPA, these results support the idea that ATX and LPA are active participants in lymphocyte trafficking, presumably regulating lymphocyte migratory behaviors locally at HEVs.

Materials and Methods

Mice

C57BL/6J and AKR/J mice were purchased from Japan SLC (Hamamatsu, Japan) and CLEA Japan (Tokyo, Japan), respectively. NOD and GFP-transgenic mice[18] were kind gifts from Dr. J. Miyazaki (Division of Stem Cell Regulation Research, Osaka University, Osaka, Japan) and Dr. M. Okabe (Research Institute of Microbial Diseases, Osaka University), respectively. The following genetically engineered and mutant mice were backcrossed on a C57BL/6J background for at least four generations, and the backcrossed progeny were used in experiments at 6 to 12 weeks of age: $CCR7^{-/-}$,[19] $DOCK2^{-/-}$,[20] $TLR2^{-/-}$,[21] $TLR4^{-/-}$,[21] $MyD88^{-/-}$,[21] $CXCL13^{-/-}$,[22] and *plt/plt*.[23] Mice were housed at the Institute of Experimental Animal Sciences at Osaka University Medical School, and the experimental protocols were approved by the Ethics Review Committee for Animal Experimentation of the Osaka University Graduate School of Medicine.

Cells and Reagents

$MAdCAM\text{-}1^+$ HEV ECs were purified from pooled mesenteric LNs as described.[24] The mouse capillary EC line, MBEC4[25] was maintained in Dulbecco's modified Eagle's medium (DMEM) supplemented with 2 mmol/L L-glutamine, 100 U/ml penicillin, 100 μg/ml streptomycin, 10% fetal calf serum (FCS), 1 mmol/L sodium pyruvate, 10 mmol/L HEPES, 0.1 mmol/L nonessential amino acids, and 50 μmol/L 2-mercaptoethanol. To establish cells stably expressing ATX, MBEC4 cells were co-transfected with a mixture of two plasmids, mlysoPLDpCAGGS[26] and pSV2-neo, carrying the neomycin (G418) resistance gene, and grown in DMEM containing 750 μg/ml of G418 (Sigma, St. Louis, MO). Individual G418-resistant clones were isolated by limiting dilution and screened by Western blotting and immunocytochemistry with an anti-ATX mAb (4F1)[14] and by measuring the lysoPLD activities of the culture media. Fatty acid-free bovine serum albumin (BSA), 1-oleoyl-LPC, and Ki16425 were purchased from Sigma. LPA (1-oleoyl-2-hydroxy-sn-3-glycerol-3-phosphate) was purchased from Biomol International (Plymouth Meeting, PA).

Quantitative Real-Time Reverse Transcriptase-Polymerase Chain Reaction (RT-PCR)

Total RNA was isolated from various tissues using Isogen (Nippongene, Toyama, Japan) and reverse-transcribed using the Super-Script first-strand synthesis system for RT-PCR (Invitrogen, Carlsbad, CA). Oligonucleotide primers for PCR were designed using Primer Express Software (Applied Biosystems, Foster City, CA). The sequences of the oligonucleotides used in PCR were as follows: ATX (mouse), forward, 5′-GGAGAATCACACTGGGTAGATGATG-3′; ATX (mouse), reverse, 5′-ACGGAGGGCGGACAAAC-3′; GAPDH, forward, 5′-GCCAAGGTCATCCATGACAACT-3′; GAPDH, reverse, 5′-GAGGGGCCATCCACAGTCTT. PCR reactions were performed using an ABI Prism 7000 sequence detection system (Applied Biosystems). The transcript number of GAPDH was quantified, and each sample was normalized on the basis of GAPDH content.

Immunohistochemistry

Formalin-fixed, paraffin-embedded sections (4 μm) were dewaxed, rehydrated, and boiled in 10 mmol/L citrate buffer, pH 6.0. Sections were then washed in Tris-buffered saline and incubated with anti-ATX mAb (4F1) and anti-PNAd mAb (MECA-79)[27] or anti-MAdCAM-1 mAb

(MECA-89)[28] at 4°C overnight, followed by biotin-conjugated goat anti-rat IgG + IgM (Southern Biotechnology Associates, Inc., Birmingham, AL). The sections were further incubated with horseradish peroxidase-conjugated ABC reagent (Vectastain ABC-HRP kit; Vector Laboratories, Burlingame, CA), developed with Metal Enhanced DAB (Pierce, Rockford, IL), and counterstained with Mayer's hematoxylin (Muto Pure Chemicals Co., Tokyo, Japan). In some experiments, biotin-labeled tyramide reagent (Perkin-Elmer Life Sciences, Boston, MA) was used for signal amplification.

PCR Analysis

Total RNA was extracted from mesenteric LNs using TRIzol (Invitrogen). Single-strand cDNA synthesized using the Ready-To-Go kit (GE Health Care UK Ltd., Amersham Place, UK) and a cDNA library of MAdCAM-1$^+$ HEVs[29] were used in PCR analysis with Ex-TaqDNA polymerase (Takara Bio, Otsu, Japan). PCR was performed at 94°C for 2 minutes, 38 cycles at 94°C for 30 seconds, at 57°C for 30 seconds, at 72°C for 30 seconds, and a final extension at 72°C for 5 minutes. The following primer pairs were used: ATX: sense, 5′-TCTAGCATCCCAGAGCACCT-3′, antisense, 5′-GGTCGGTGAGGAAGGATGAA-3′; LPA_1: sense, 5′-AAGCAAGCATGTGGTGTGTG-3′, antisense, 5′-ATGTCTATAGGCATACGTGG-3′, LPA_2: sense, 5′-GCTAGTACTGAAGCTGATTCC-3′, antisense, 5′-AGCCTAGTCTATGCGGCAAG-3′; LPA_3: sense, 5′-GATGAGAGTCCACAGCAACTTG-3′, antisense, 5′-AGATGCGTACGTATACCGCC-3′[30]; and LPA_4: sense, 5′-CACATATAAGGATGGAGTCGC-3′, antisense, 5′-GTCAACTCAACAGAAGAGGC-3′; CD3ε: sense, 5′-CCTGACAGCAGTAGCCATAATC-3′, antisense, 5′-GCTGTTGAGTCAGCAATGTCC-3′; L-selectin: sense, 5′-GCCATGGTGTTTCCATGGAGATGTGAGGGT-3′, antisense, 5′-ATCATCCATCCTTTCTTGAGATTTCTTGCC-3′; β-actin: sense, 5′-ATGGATGACGATATCGCT-3′, antisense, 5′-ATGAGGTAGTCTGTCAGGT-3′. PCR products were analyzed by agarose gel electrophoresis.

In Situ *Hybridization Assay*

Plasmids (pCRII; Invitrogen) containing cDNA fragments of LPA_1 (500 bp), LPA_4 (366 bp), or MAdCAM-1 (482 bp) were used as templates for RNA probe synthesis. Digoxigenin (DIG)-labeled antisense or sense probes were prepared with T7 and SP6 RNA polymerase (Applied Biosystems), respectively, using the DIG RNA labeling mix (Roche Diagnostics, Basel, Switzerland). Mesenteric and peripheral LNs were fixed with 4% paraformaldehyde for 2 hours, incubated in 30% sucrose in phosphate-buffered saline (PBS) overnight, and embedded in OCT compound. Eight-μm-thick serial frozen sections were fixed in 4% paraformaldehyde for 20 minutes, incubated in 0.1% H_2O_2, and permeabilized with 50 μg/ml proteinase K for 5 minutes. After an additional fixation with paraformaldehyde, the sections were treated with acetic anhydride in triethanolamine for 10 minutes. The sections were then prehybridized with 50% formamide, 5× standard saline citrate, 1 mg/ml yeast tRNA (Roche Diagnostics), 100 μg/ml heparin, 1× Denhardt's solution, and 0.1% Tween 20 at 60°C for 3 hours, and then hybridized with labeled probe in the same solution overnight at 60°C. After being washed, the sections were incubated with horseradish peroxidase-conjugated anti-DIG (Roche Diagnostics), followed by biotin-labeled tyramide (TSA Biotin System, PerkinElmer Life Sciences) for signal amplification. The hybridized probes were then detected by ABC-alkaline phosphatase (Vector Laboratories) and NBT/BCIP (Roche Diagnostics).

Fluorescence Microscopy

Purified MAdCAM-1$^+$ HEV ECs were seeded in collagen type 1-coated eight-well culture slides (Becton Dickinson, Mountain View, CA) (4×10^4 cells/well) and incubated for 3 hours in DMEM containing 20% FCS (Hyclone, Logan, UT). After the nonadherent cells were removed, the remaining ECs were treated for 60 minutes with LPA (15 μmol/L) in fresh DMEM containing FCS stripped with 10% charcoal. Similarly, MBEC4 cells and ATX-expressing MBEC4 cells were seeded in Lab-Tek II chamber slides (Nalge Nunc, Rochester, NY) (0.5×10^4 cells/well), cultured overnight, and treated for 60 minutes with LPA or LPC (10 μmol/L) in fresh DMEM containing 0.1% fatty acid-free BSA. In some experiments, cells were pretreated with 10 μmol/L Ki16425 (Sigma) for 60 minutes at 37°C. After two washes in PBS, the cells were fixed in 4% paraformaldehyde, permeabilized in PBS containing 0.1% Triton X-100, and incubated with Alexa Fluor 594-conjugated MECA89 (2 μg/ml) followed by Alexa Fluor 488-phalloidin (1 U/ml) (Invitrogen) (for MAdCAM-1$^+$ HEV ECs) or Alexa Fluor 488-phalloidin alone (for MBEC4 and ATX-expressing MBEC4 cells). The cells were then observed under a confocal microscope (LSM510META; Carl Zeiss, Jena, Germany; or Radiance 2100; Bio-Rad, Hercules, CA) using Fluoromount-G mounting medium (Southern Biotechnology).

Lymphocyte Binding Assay

Freshly isolated MAdCAM-1$^+$ HEV ECs, MBEC4, and ATX-expressing MBEC4 cells were cultured and stimulated as follows. The MAdCAM-1$^+$ HEV ECs were plated (2.5×10^4 cells/well) in collagen-coated 96-well plates (Becton Dickinson) and allowed to adhere for 3 hours in DMEM containing 20% FCS (Hyclone). After the unbound cells were removed, the remaining cells were starved for 60 minutes by incubation in DMEM containing 0.1% fatty acid-free BSA. MBEC4 cells and MBEC4 transfectants expressing ATX were plated in a flat-bottomed 96-well plate (1×10^4 cells/well) and grown in DMEM containing 10% FCS overnight. The cells were then starved for 16 hours by incubation in DMEM with 0.1% fatty acid-free BSA. These EC preparations were incubated with or without various concentrations of LPA or LPC for 30 to 60 minutes in DMEM with 0.1% fatty acid-free BSA, as indicated. For inhibition studies, the ECs were pretreated with 10 μmol/L Ki16425 for 30 minutes. Spleen cells that

did not adhere to plastic were labeled with the fluorescent indicator BCECF-AM as described,[31] in DMEM with 0.1% fatty acid-free BSA. They were then added to the wells containing the ECs (5×10^5 cells/well) and allowed to bind to the ECs for 30 minutes under static conditions or with rotation (120 rpm). Unbound lymphocytes were removed by inverting the plate, which had been filled with prewarmed FCS-free RPMI 1640 and sealed with Parafilm (Pechinery Plastic Packaging, Inc., Menasha, WI) for 30 minutes at room temperature. The adherent lymphocytes were solubilized with 1% Nonidet P-40 in PBS, and fluorescence intensity was measured by a fluorescence enzyme-linked immunosorbent assay reader (SpectraMax Gemini XS; Molecular Devices, Sunnyvale, CA).

Short-Term Homing Assay

The lymphocyte migration assay was performed as previously described.[22] Briefly, spleen cells obtained from GFP-transgenic mice were injected intravenously into mice (2×10^7 cell/mouse) that had received an intraperitoneal injection of a cocktail of anti-ATX mAbs (clones 5E5, S13A9, and S9A9; 150 μg each) or rat IgG (450 μg/mouse; Cappel, Aurora, OH) 3 hours before. The mice were sacrificed 2.5 hours after the lymphocyte injection, and the spleen, mesenteric LNs, brachial LNs, and PPs were harvested. The number of lymphocytes that had migrated into these tissues was determined by flow cytometry.

LysoPLD Assay

Plasma samples (10 μl) were incubated with 4 mmol/L LPC in buffer containing 100 mmol/L Tris-HCl (pH 9.0), 500 mmol/L NaCl, 5 mmol/L $MgCl_2$, and 0.05% Triton X-100 for 12 hours at 37°C. The liberated choline was detected by an enzymatic photometric method using choline oxidase (Asahi Chemical Industry, Tokyo, Japan), horseradish peroxidase (Toyobo, Tokyo, Japan), and TOOS reagent [*N*-ethyl-*N*-(2-hydroxy-3-sulfopropyl)-m-toluidine] (Dojin, Tokyo, Japan), as reported previously.[32] Absorbance was read at 560 nm and converted to nanomoles of choline by comparison to a choline standard curve.

Statistical Analysis

A Student's *t*-test was applied to compare the statistical difference within two groups.

Results

ATX Is Constitutively and Selectively Expressed in HEVs of Peripheral and Mesenteric LNs and PPs

Preliminary analysis showed that ATX transcripts appeared at moderate frequencies in the previously generated 3′-directed cDNA libraries of $PNAd^+$ HEV ECs[24] and of MAdCAM-1^+ HEV ECs[33]; they appeared five times among 1558 transcripts obtained from the $PNAd^+$ HEV cDNA library and five times among 2101 transcripts in the MAdCAM-1^+ HEV cDNA library. Transcripts of endoglin were found at comparable frequencies in these libraries (data not shown). ATX transcripts are also found in a human tonsil cDNA library enriched for HEV-derived cDNAs by subtraction with lymphocyte cDNAs and umbilical vein endothelial cDNAs.[16] Real-time PCR analysis showed that ATX mRNA was strongly expressed in the peripheral and mesenteric LNs as well as in the brain and kidney among the mouse tissues tested (Figure 1A). These findings prompted us to look for the expression and localization of ATX proteins in HEVs. As shown in Figure 1B, specific mAb against ATX readily detected its expression in HEVs of peripheral and mesenteric LNs and PPs, but not in non-HEV blood vessels in experimentally naïve mice. Although staining intensities varied in different HEVs, a majority of HEVs of LNs appeared positive for ATX expression, whereas ~30 to 40% of HEVs of PPs expressed ATX. In mesenteric LNs, both $PNAd^+$ HEVs and MAdCAM-1^+ HEVs expressed ATX (Figure 1C).

We next examined ATX expression in developing LNs. Although ATX expression was not observed prenatally (Figure 2A), it was detectable 1 day after birth (Figure 2B), and its level increased progressively until postnatal day 7 (Figure 2, C and D), concomitant with the increasing numbers of lymphocytes around HEVs in the peripheral and mesenteric LNs. The appearance of ATX also paralleled to that of PNAd in peripheral LNs (data not shown).[34]

ATX Expression Is Up-Regulated in Venules at Sites of Chronic Inflammation

HEV-like venules appear in sites other than peripheral and mesenteric LNs and PPs under certain pathological conditions. For instance, a marked increase in lymphocyte trafficking is associated with the appearance of HEV-specific adhesion molecules and a HEV-like morphology in the cortico-medullary venules of the thymus in aged AKR/J mice that develop thymic hyperplasia and lymphoma.[35,36] We found that a majority of the cortico-medullary venules of hyperplastic thymus from old (>30 weeks) AKR/J mice were $PNAd^+$, as revealed by mAb MECA-79 staining, and ~60 to 70% of the $PNAd^+$ venules were also positive for ATX expression (Figure 3A). Most of the ATX^+ venules appeared $PNAd^+$ (Figure 3A). In contrast, a majority of the thymic venules of young AKR/J mice (6 to 8 weeks old) and 30-week-old C57BL/6 mice were PNAd-negative (date not shown), although a small fraction of C57BL/6 mice (<20 ~ 30%) showed weak but distinct ATX expression in these venules at 6 to 8 weeks of age (Figure 3B). A previous study showed that insulitis in NOD mice is associated with the occurrence of HEV-like vessels bearing PNAd epitopes.[37] Our study confirmed this observation and showed that a substantial proportion of the $PNAd^+$ venules in the pancreas of the NOD mice were also positive for ATX, whereas the venules of uninflamed islet tissues in the NOD mice were

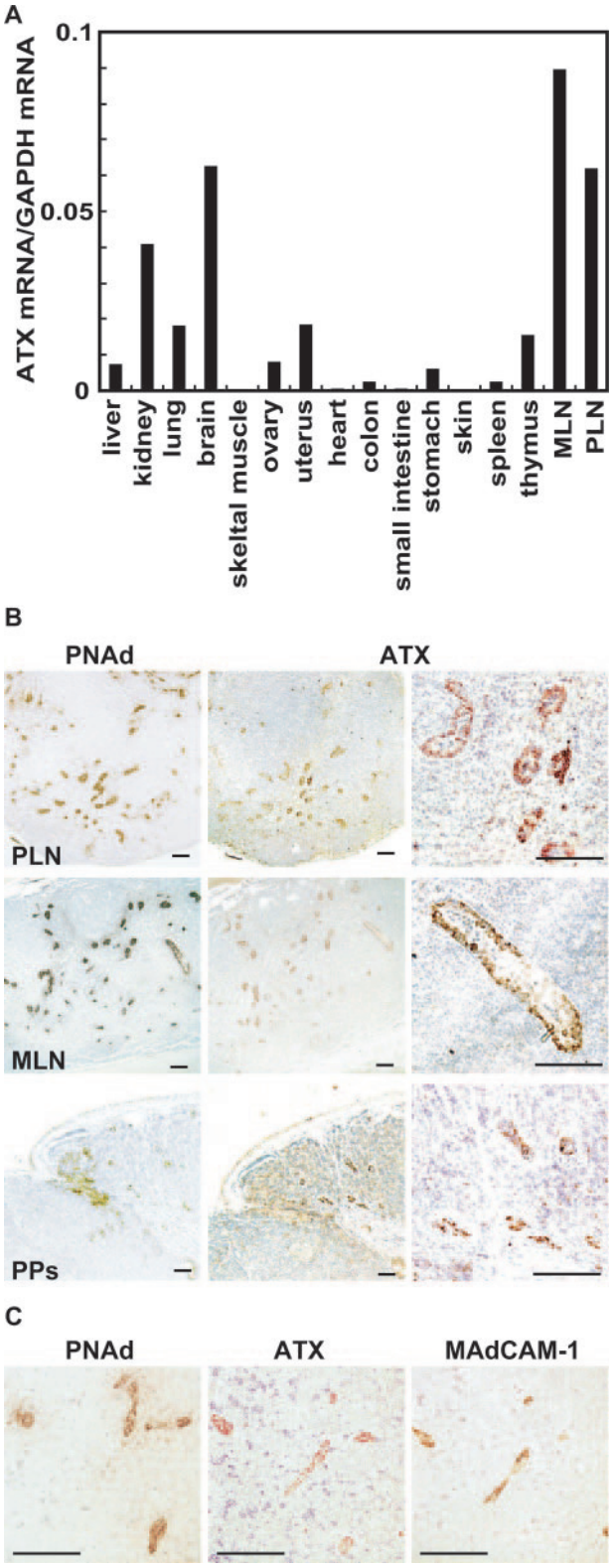

Figure 1. ATX is selectively expressed in HEVs of LNs and PPs. **A:** ATX mRNA expression was examined in various mouse tissues by real-time PCR. The abundance of ATX mRNA was normalized by GAPDH mRNA control. **B:** Serial paraffin sections of peripheral LNs (LN; **top**), mesenteric LNs (MLN; **middle**), and PPs (**bottom**) from wild-type mice incubated with MECA-79 mAb (**left**) or anti-ATX/lysoPLD mAb (**middle** and **right**). **C:** Serial sections of mesenteric LNs incubated with anti-PNAd, anti-ATX, or anti-MAdCAM-1, and stained as in **A**. Scale bars = 100 μm.

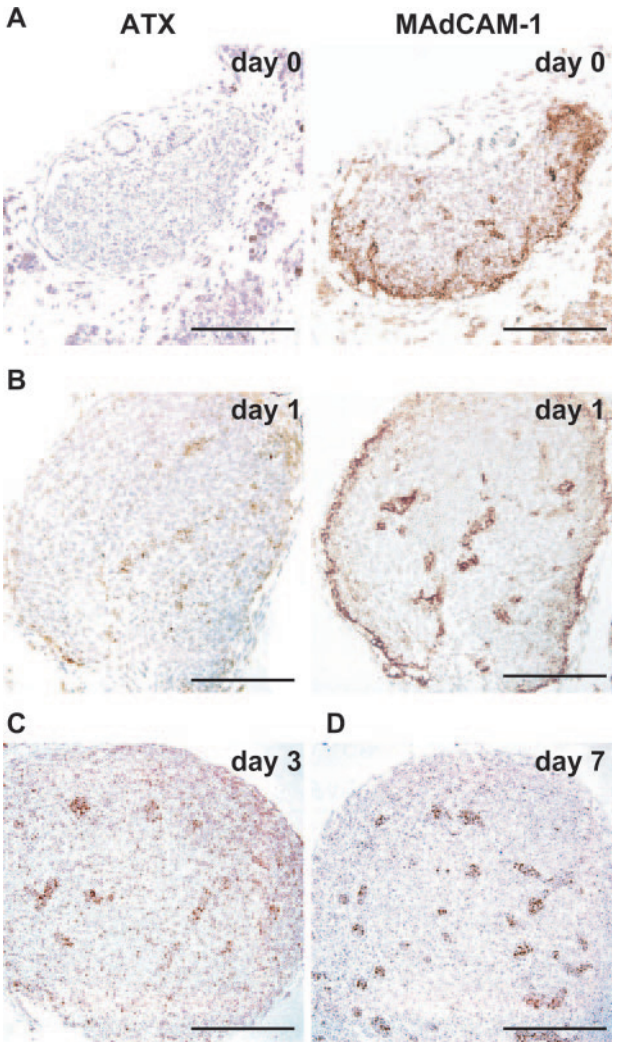

Figure 2. ATX expression appears in HEVs on day 1 after birth and is up-regulated subsequently in HEVs. **A** and **B:** Serial paraffin sections of peripheral LNs from neonates on day 0 (**A**) and day 1 (**B**) incubated with anti-ATX mAb or anti-MAdCAM-1 mAb. **C** and **D:** Paraffin sections of peripheral LNs from day 3 (**C**) and day 7 (**D**) stained with anti-ATX mAb as above. Without anti-ATX mAb, some stromal cells in the developing LNs gave nonspecific signals. Scale bars = 100 μm.

negative for PNAd and ATX (Figure 3C). These observations are in agreement with the hypothesis that ATX plays a role in lymphocyte trafficking into chronically inflamed tissues.

The Expression of ATX Is Independent of Signals Mediated by Lymphoid Chemokines (CCL21 and CXCL13), DOCK2, or MyD88

We next addressed the regulatory mechanism of ATX expression. To this end, we first investigated ATX expression in the HEVs of CCR7-deficient mice,[19] *plt/plt* mice,[23] and CXCL13-deficient mice,[22] all of which show substantially reduced lymphocyte homing. In addition, we examined mice deficient in DOCK-2, which plays an essential role in CCR7- and CXCR5-mediated signaling[20]; DOCK-2-deficient mice also show severely impaired lymphocyte

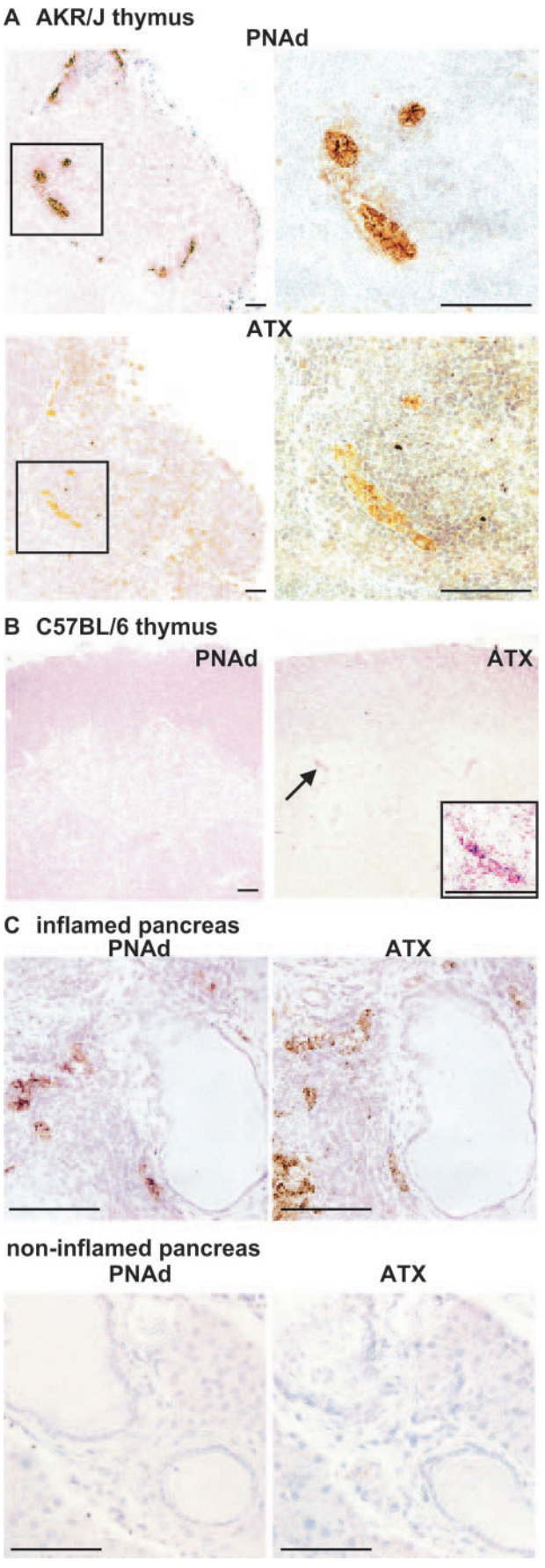

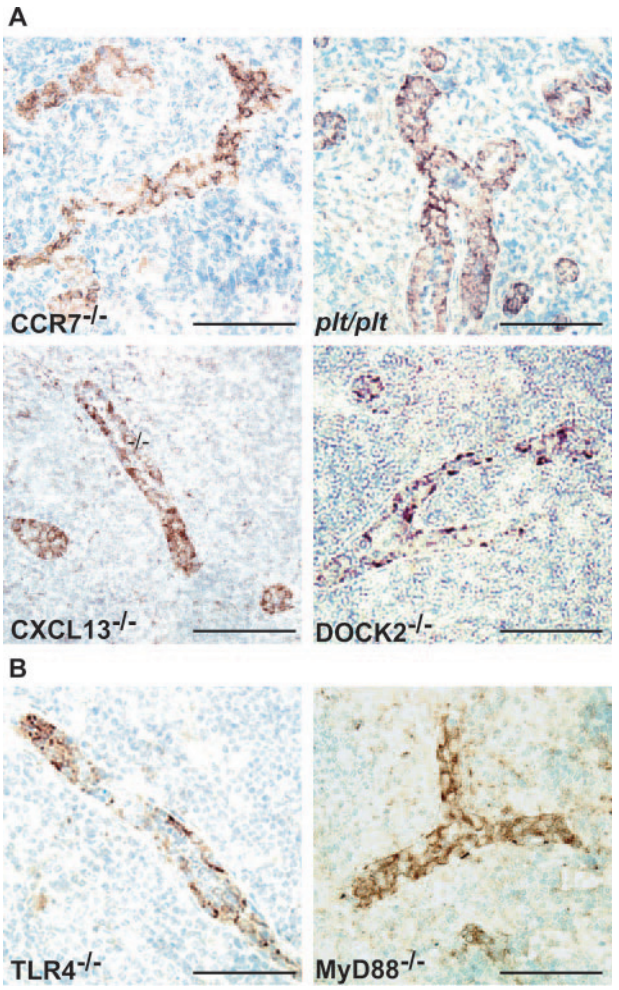

Figure 4. The expression of ATX is independent of lymphoid chemokine (CCL19/21 and CXCL13)-, DOCK2-, or MyD88-mediated signals. Anti-ATX staining of paraffin sections of mesenteric LNs from CCR7$^{-/-}$, CXCL13$^{-/-}$, DOCK2$^{-/-}$, or *plt/plt* mice (**A**) and TLR4$^{-/-}$ or MyD88$^{-/-}$ mice (**B**). Scale bars = 100 μm.

trafficking to LNs. All of the mice examined were 6 to 12 weeks old. We saw no differences in ATX expression in the HEVs of the CCR7-deficient, CXCL13-deficient, *plt/plt*, or DOCK-2-deficient mice, compared with wild-type mice, indicating that lymphocyte trafficking across HEVs per se does not affect ATX expression in these venules (Figure 4A). These results also indicate that ATX expression is independent of lymphoid chemokines, such as CCL21 and CXCL13, and of CCR7-dependent signals in the HEVs of adult animals.

Given that HEVs express TLR4 (M. Kiyomi and T. Tanaka, unpublished observation), which induces a spe-

Figure 3. ATX expression is up-regulated in venules of AKR hyperplastic thymus and in chronically inflamed blood vessels in the NOD pancreas. **A** and **B:** Serial paraffin sections of hyperplastic thymus from aged AKR/J mice (**A**) and thymus of normal mice (**B**) incubated with anti-PNAd mAb (**A: top**) or anti-ATX mAb (**A: bottom**). In **A**, the **right panel** shows a higher magnification view of the boxed area at **left**. In **B**, **right panel**, boxed region shows higher magnification view of ATX expression near the cortico-medullary junction in wild-type mouse thymus (indicated by **arrow** at low magnification). **C:** Serial paraffin sections of inflamed (**top**) and noninflamed (**bottom**) pancreas from NOD mice incubated with anti-PNAd mAb or anti-ATX mAb, as indicated. Scale bars = 100 μm.

cific differentiation program in certain cell types on its ligation,[38] we next examined whether ATX expression is under the control of TLR signaling. In mice deficient for TLR4 or MyD88, which mediates signaling by many of the TLRs,[21] there was no noticeable difference from wild-type in ATX expression (Figure 4B), which is incompatible with the idea that TLR signaling regulates ATX expression in HEVs. These results also indicate that innate immunity signals mediated by TLR4 and MyD88 are dispensable for ATX expression in HEVs.

HEV ECs Express Specific Receptors for LPA and Show Cytoskeletal Changes by LPA Stimulation

Although ATX can generate LPA[12,39] and S1P[13] from their respective precursors *in vitro*, recent studies indicate that ATX is the major LPA-producing enzyme *in vivo*.[14,40] Therefore, to investigate whether LPA could act through a paracrine or autocrine mechanism at the HEV EC surface, we next examined LPA receptor expression in HEV ECs. We found that MAdCAM-1$^+$ HEV ECs obtained from mesenteric LNs expressed LPA_1 and LPA_4, and that unfractionated mesenteric LN cells consisting mainly of lymphocytes expressed readily detectable levels of LPA_1, LPA_2, LPA_3, and a low level of LPA_4 at the mRNA level (Figure 5A). Importantly, the possibility that contaminating lymphocytes were responsible for the expression of the LPA receptors in the HEV EC preparation was ruled out because the EC preparation used here showed no signal for CD3ε or L-selectin mRNA, whereas the mesenteric LN cells showed strong CD3ε and L-selectin mRNA signals. The LPA receptor expression by HEV ECs was also verified by *in situ* hybridization analysis. As shown in Figure 5B, MAdCAM-1-expressing HEV ECs showed strong signals when hybridized with antisense probes for LPA_1 and LPA_4, but not with sense probes for these receptors. These findings collectively indicate that HEV ECs express LPA_1 and LPA_4.

We next examined the function of LPA receptors expressed by HEV ECs. Given that ATX is constitutively expressed in HEV ECs, one possible role for this cell-motility protein is to induce the local production of LPA in HEVs, which could function in turn as an autocrine or paracrine factor for the HEV ECs and/or lymphocytes. To test this possibility, we added LPA to HEV ECs *in vitro* and found by confocal imaging that the HEV ECs showed prominent morphological changes in response to the exogenous LPA (Figure 5C); ~50% of HEV ECs showed extended cell morphology with actin-rich cell protrusions and cell-surface ruffling, and this change was almost completely inhibited by Ki16425, which antagonizes at least LPA_1 and LPA_3, if not other isoforms.[41]

We also examined the effect of LPA and LPC on lymphocyte binding to HEV ECs. However, because purified HEV ECs showed high endogenous lymphocyte binding in the absence of any deliberate stimulation *in vitro*,[24,33] we could not determine the effect of LPA or LPC on lymphocyte binding in this experimental setup. Therefore, to further examine this issue, we resorted to using ATX-expressing cultured ECs that bind lymphocytes only moderately.

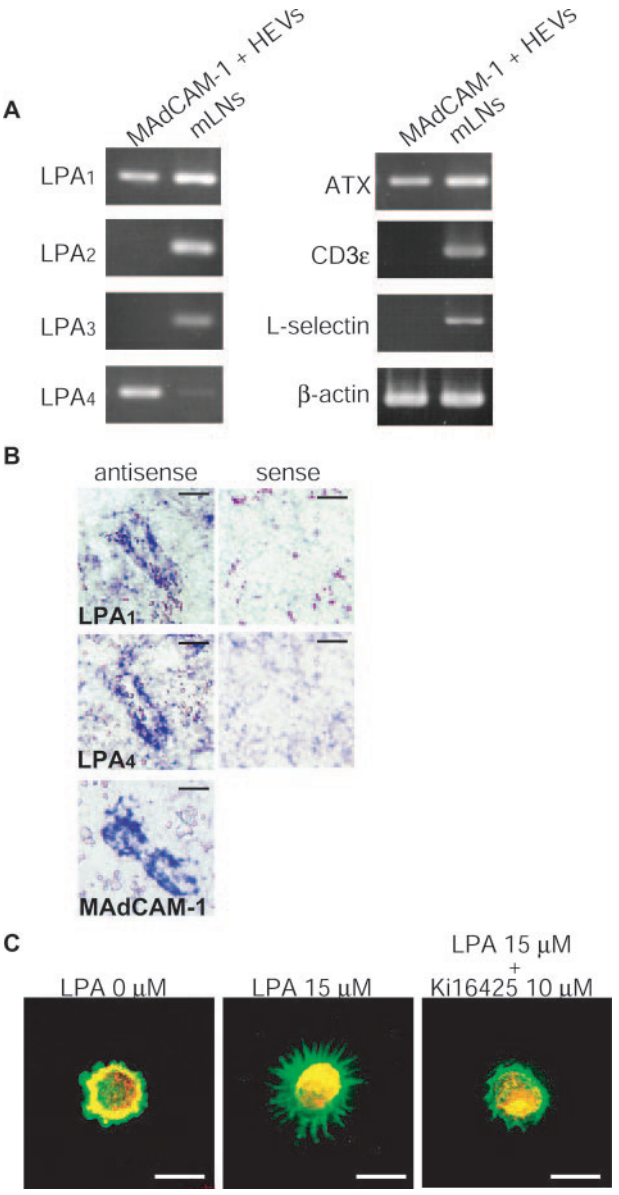

Figure 5. HEV ECs express LPA receptors and show cytoskeletal changes in response to LPA. **A:** LPA_{1-4}, ATX, CD3ε, and L-selectin mRNA expression analyzed by RT-PCR. mRNAs expressed in HEV cDNA libraries (MAdCAM-1$^+$ HEVs) and mesenteric LNs were analyzed. β-Actin was the positive control. **B:** *In situ* hybridization analysis of LPA_1, LPA_4, and MAdCAM-1 mRNAs. Sections of mesenteric LNs were hybridized with DIG-labeled sense or antisense riboprobes as indicated. **C:** Adherent HEV ECs, control or stimulated with 15 μmol/L LPA, were stained with Alexa Fluor 594-conjugated MECA89 and Alexa Fluor 488-phalloidin. For inhibition studies, HEV ECs were pretreated with 10 μmol/L Ki16425, an LPA_1 and LPA_3 antagonist. Scale bars: 100 μm (**B**); 50 μm (**C**).

Forced Expression of ATX by Cultured ECs Confers Responsiveness to LPC

To generate cultured EC lines constitutively expressing both ATX and LPA receptors, we introduced an expression vector for ATX into an EC line, MBEC4, that endog-

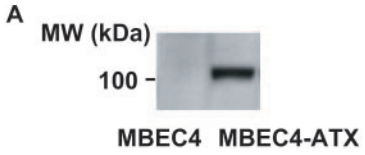

Figure 6. LPC induced morphological changes in ATX-expressing ECs and enhanced lymphocyte binding to them. **A:** Expression of ATX in MBEC4-ATX cells analyzed by Western blotting. MW, molecular weight. Essentially all MBEC4-ATX cells (>98%) were positive for ATX expression and they produced biologically active ATX with lysoPLD activity (241.8 nmol/ml/hour in 100-hour conditioned medium). **B:** MBEC4 or MBEC4-ATX cells incubated with or without 10 μmol/L LPA or LPC were fixed, permeabilized, and stained with Alexa Fluor 488-phalloidin. For inhibition studies, cells were pretreated with 10 μmol/L Ki16425, an LPA_1 and LPA_3 antagonist. **C** and **D:** MBEC4-ATX and MBEC4 incubated with or without various concentrations of LPA or LPC to which BCECF-labeled lymphocytes were added without (**C**) or with continuous rotation (120 rpm) (**D**). The adherent lymphocytes were solubilized and quantified by a fluorescence plate reader. For inhibition studies, these cells were pretreated with Ki16425. Data represent the mean ± SD for three separate experiments. *, ***$P < 0.005$ compared with vehicle-treated MBEC4-ATX cells. **, ****$P < 0.005$ compared with vehicle-treated MBEC4 cells.

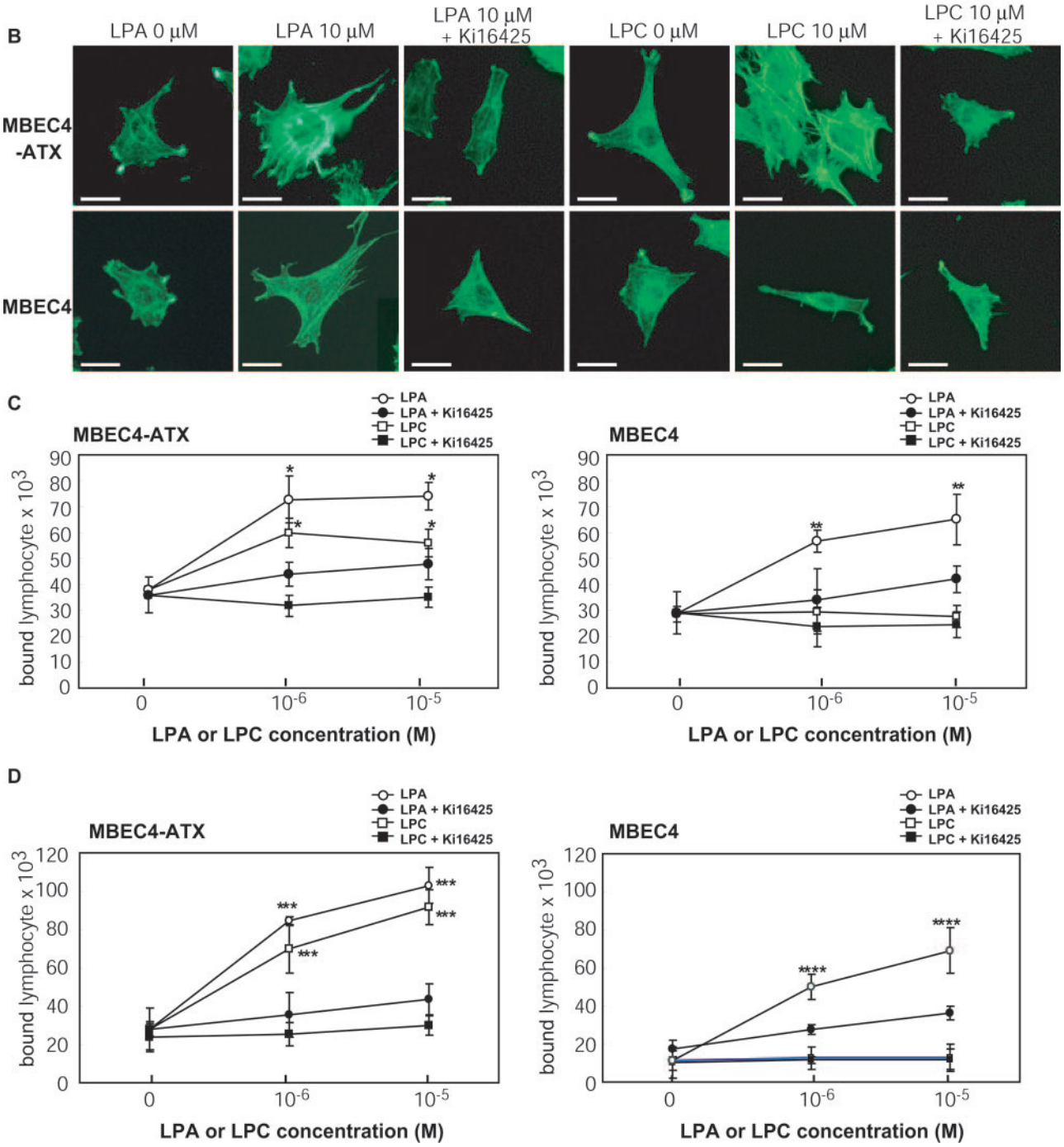

enously expresses receptors for LPA, and determined the cells' responses to LPA and LPC. As shown in Figure 6A, the ATX-transfected MBEC4 cell lines (MBEC4-ATX) expressed ATX abundantly, whereas the parental MBEC4 ECs did not express ATX. The MBEC4-ATX cells showed strong morphological changes in response to LPA and LPC (~70% of cells showed extended cell morphology with well-developed stress fibers), and these

changes were inhibited by Ki16425 (Figure 6B). In contrast, the parental MBEC4 cell line responded to LPA but not to LPC. These results are in agreement with the hypothesis that ECs producing high levels of ATX respond not only to LPA but also to LPC by converting LPC to LPA, whereas ATX-negative cells respond to LPA but not to LPC, because they are incapable of hydrolyzing LPC to LPA.

Differential effects by LPA and LPC on lymphocyte binding to these EC lines were also observed (Figure 6C). The MBEC4-ATX cells showed increased lymphocyte binding when exposed to 1 to 10 μmol/L LPA or LPC under static conditions. In contrast, the MBEC4 cells showed increased lymphocyte binding in response to 1 to 10 μmol/L LPA but not LPC. Under continuous rotation (120 rpm), the MBEC4-ATX showed increased lymphocyte binding in the presence of LPC, whereas the parental MBEC4 cells did not (Figure 6D). These results further support the hypothesis that endothelial ATX promotes the motility of lymphocytes and ECs by converting LPC to LPA on the EC surface.

Depletion of ATX from the Circulation Does Not Impair Lymphocyte Trafficking to Secondary Lymphoid Tissues

ATX is a type-II transmembrane protein that undergoes membrane-proximal cleavage to yield a soluble lysoPLD that is released into the plasma.[42] To address the functional roles of ATX in regulating lymphocyte trafficking *in vivo*, we attempted to deplete the circulating ATX by injecting a cocktail of anti-ATX mAbs intraperitoneally into mice. This injection successfully depleted ATX from the plasma, decreasing the plasma lysoPLD activity to ~10% of that seen in mice given a control rat IgG (Figure 7A). However, lymphocyte trafficking to the spleen, brachial LNs, mesenteric LNs, and PPs in the anti-ATX-treated mice, as examined by adoptive transfer of fluorescently labeled lymphocytes, was comparable to the trafficking observed in the control mice (Figure 7B). These observations suggest that the ATX in the general circulation does not play a major role in lymphocyte trafficking to secondary lymphoid tissues but argues for the role of ATX in the local environment; given that ATX is selectively expressed in HEVs and that endothelial ATX promotes the motility of lymphocytes and ECs as shown above, these findings are compatible with the idea that ATX regulates lymphocyte-endothelial interactions not systemically but locally at HEV.

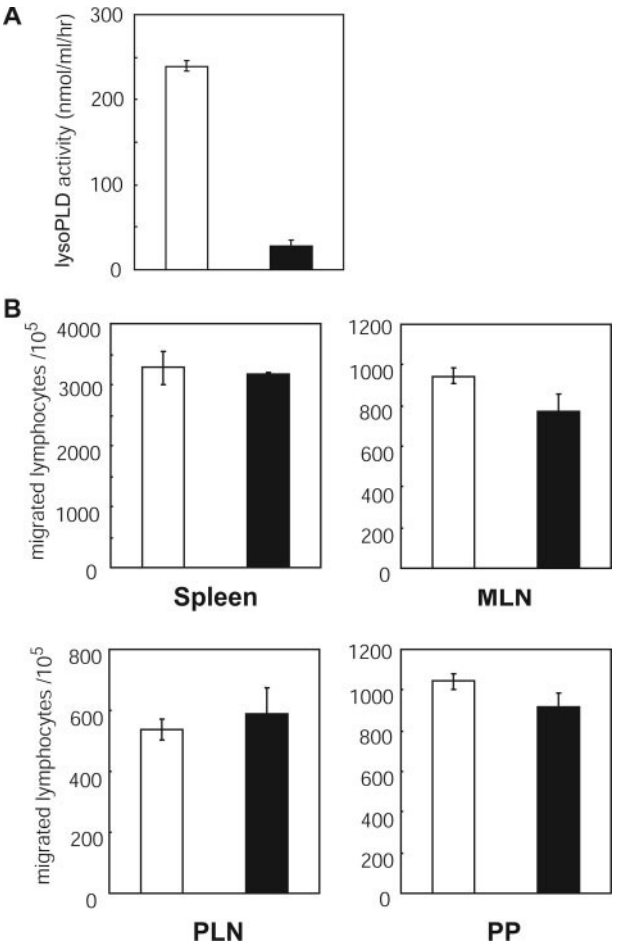

Figure 7. Circulating ATX does not contribute to lymphocyte trafficking to secondary lymphoid tissues, including spleen, LNs, and PPs. **A:** Mice were treated with either control rat IgG (white bar) or anti-ATX mAb (black bar), and LysoPLD activity in mouse plasma was determined by the liberation of choline from LPC 5.5 hours after injection of a cocktail of anti-ATX mAbs. **B:** Short-term lymphocyte homing assay performed. GFP-expressing mouse spleen cells were injected intraperitoneally into mice treated with either control or anti-ATX antibodies 3 hours previously. The numbers of lymphocytes that migrated into spleen, mesenteric LNs (MLNs), peripheral LNs (PLNs), and PPs were quantified by flow cytometry 2.5 hours after the lymphocyte injection.

Discussion

In this study, we addressed the biological role of ATX expressed by HEVs. ATX expression was abundant in adult HEVs but scarce in the HEVs of newborns. In the developing LNs, ATX expression rapidly increased postnatally in parallel with PNAd expression, and was concomitant with the appearance of numerous lymphocytes around the HEVs. Although not expressed in intact venules of nonlymphoid tissues, ATX appeared in certain venules of chronically inflamed tissues, such as the pancreatic venules of NOD mice and the thymic venules of AKR mice, which expressed the L-selectin-reactive PNAd epitope and showed prominent perivascular lymphocyte infiltration. In contrast, ATX was absent from blood vessels in these tissues that showed no perivascular lymphocyte infiltration. Thus, ATX expression was always positively correlated with lymphocyte trafficking across venules, strongly implicating ATX in this phenomenon.

Kanda and colleagues[17] recently published a study in which they showed that ATX, secreted by HEVs, binds to the chemokine-activated lymphocytes and generated LPA, which in turn enhances lymphocyte motility through Gαi-coupled receptors. They also showed that intravenous injection of an enzymatically inactive form of ATX blocked the trafficking of blood lymphocytes to LNs, PPs, and spleen.[17] Our *in vitro* observations also support a functional role for ATX in lymphocyte-HEV interactions.

Because ATX is a major producer of LPA,[14] we hypothesized that ATX generates LPA from its precursor LPC and that LPA may act on not only lymphocytes but also HEV ECs in an autocrine and/or paracrine manner, because both cells express LPA receptors. Consistent with this idea, HEV ECs expressed LPA_1 and LPA_4, and although the effect of LPA and LPC on lymphocyte binding to HEV ECs could not be determined because of a high background lymphocyte binding, the HEV ECs showed increased cell-surface ruffling and pseudopod extension in response to exogenous LPA, which was abrogated by Ki16425, indicating that LPA enhances the motility of HEV ECs, which may facilitate physical encounters and subsequent interactions with lymphocytes *in situ*. In addition, when ATX-expressing cultured ECs were used, it was notable that pretreatment with not only LPA but also LPC increased the lymphocyte binding to ATX-expressing ECs under static as well as flow conditions. In contrast, only LPA (not LPC) increased lymphocyte binding in ATX-negative ECs. These observations support the idea that ECs producing high levels of ATX respond to LPA and also to LPC and that endothelial ATX enhances the motility of lymphocytes and ECs by converting LPC to LPA on the HEV EC surface locally. Whether ATX has an effect on lymphocyte binding to HEVs could be finally resolved by *in situ* application of ATX inhibitors, such as neutralizing anti-ATX monoclonal antibodies, which are as yet unavailable, to HEVs.

Given that ATX is expressed in restricted cell types *in vivo*, its expression must be regulated rigorously. Although transcriptional regulation is likely to be one mechanism for this, we do not know what molecules are involved in regulating the transcription of ATX. Our experiments with mice genetically deficient in CXCL13, DOCK-2, CCR7, TLR4, or MyD88, and with *plt/plt* mice, indicated that neither signals from lymphoid chemokines, such as CCL21 and CXCL13, nor the TLR4 are involved in the regulation of ATX expression. Lymphocyte trafficking itself did not appear to be involved in this process either.

Whereas the above-mentioned results are compatible with the idea that ATX is involved in the up-regulation of lymphocyte-HEV interactions by generating LPA locally, we found that the systemic depletion of ATX did not affect lymphocyte trafficking into the LNs. This shows a contrast to the study by Kanda and colleagues[17] in which they showed that enzymatically inactive ATX injected intravenously had an inhibitory effect on short-term lymphocyte trafficking to lymphoid tissues. This discrepancy might be at least in part attributable to the fact that the mutant ATX is much smaller in size and probably penetrates into tissue parenchyma more readily than antibodies. Given that ATX is produced by limited cell types *in vivo*, we envisage that ATX acts locally at the surface of these cells, and the circulating level of ATX may be irrelevant to ATX's function *in vivo*. However, because ATX knockout mice are embryonically lethal,[14] we are currently unable to further assess the *in vivo* function of ATX at HEVs. Conditional expression or deletion of ATX in HEV ECs will be required to answer this issue.

Recent studies have shown that ATX also plays a critical role for blood vessel formation during development.[14,40] ATX-deficient embryos show severe vascular defects and die at midgestation. In the fetal stage, ATX mRNA is mainly detected in endodermal cells surrounding yolk sac and secreted ATX protein accumulates in amniotic fluid.[14] Although ATX and LPA themselves are not angiogenic *in vitro*, they can strongly promote blood vessel formation by stabilizing preformed blood vessels through currently unknown mechanisms.[14] In the adult stage, we showed that ATX is selectively expressed in HEV ECs as well as ECs of certain blood vessels in chronically inflamed tissues. This raises the possibility that ATX, in addition to stimulating cellular interactions between lymphocytes and ECs, contributes to the formation of specialized blood vessels, which support an increased lymphocyte trafficking in LNs and PPs as well as chronically inflamed tissues by regulating production of LPA *in situ*. Mechanisms underlying the selective expression of ATX in the ECs of certain blood vessels and LPA receptors responsible for vascular formation remain unknown. Further study is clearly required to resolve this issue.

Collectively, these results support the hypothesis that ATX enhances lymphocyte-HEV interactions *in vivo*. ATX may provide another layer of regulation, in addition to that by lymphoid chemokines, to the trafficking of lymphocytes across HEVs. Although it remains to be verified whether ATX mediates lymphocyte-HEV interactions via LPA, the future use of specific inhibitors of these molecules, which are not yet available, should finally elucidate the mode of action of ATX at the HEV-lymphocyte interface.

Acknowledgments

We thank Dr. Martin Lipp, Max-Delbruck-Center, for the CCR7-deficient mice; Tamae Kondo for technical support; and Shinobu Yamashita and Miyuki Komine for secretarial assistance.

References

1. von Andrian UH, Mempel TR: Homing and cellular traffic in lymph nodes. Nat Rev Immunol 2003, 3:867–878
2. Miyasaka M, Tanaka T: Lymphocyte trafficking across high endothelial venules: dogmas and enigmas. Nat Rev Immunol 2004, 4:360–370
3. Anderson ND, Anderson AO, Wyllie RG: Specialized structure and metabolic activities of high endothelial venules in rat lymphatic tissues. Immunology 1976, 31:455–473
4. Rosen H, Goetzl EJ: Sphingosine 1-phosphate and its receptors: an autocrine and paracrine network. Nat Rev Immunol 2005, 5:560–570
5. Goetzl EJ, Wang W, McGiffert C, Huang MC, Graler MH: Sphingosine 1-phosphate and its G protein-coupled receptors constitute a multifunctional immunoregulatory system. J Cell Biochem 2004, 92:1104–1114
6. Kotarsky K, Boketoft A, Bristulf J, Nilsson NE, Norberg A, Hansson S, Owman C, Sillard R, Leeb-Lundberg LM, Olde B: Lysophosphatidic acid binds to and activates GPR92, a G protein-coupled receptor highly expressed in gastrointestinal lymphocytes. J Pharmacol Exp Ther 2006, 318:619–628
7. Lee CW, Rivera R, Gardell S, Dubin AE, Chun J: GPR92 as a new

G12/13- and Gq-coupled lysophosphatidic acid receptor that increases cAMP LPA5. J Biol Chem 2006, 281:23589–23597
8. Matloubian M, Lo CG, Cinamon G, Lesneski MJ, Xu Y, Brinkmann V, Allende ML, Proia RL, Cyster JG: Lymphocyte egress from thymus and peripheral lymphoid organs is dependent on S1P receptor 1. Nature 2004, 427:355–360
9. Lo CG, Xu Y, Proia RL, Cyster JG: Cyclical modulation of sphingosine-1-phosphate receptor 1 surface expression during lymphocyte recirculation and relationship to lymphoid organ transit. J Exp Med 2005, 201:291–301
10. Cinamon G, Matloubian M, Lesneski MJ, Xu Y, Low C, Lu T, Proia RL, Cyster JG: Sphingosine 1-phosphate receptor 1 promotes B cell localization in the splenic marginal zone. Nat Immunol 2004, 5:713–720
11. Murata J, Lee HY, Clair T, Krutzsch HC, Arestad AA, Sobel ME, Liotta LA, Stracke ML: cDNA cloning of the human tumor motility-stimulating protein, autotaxin, reveals a homology with phosphodiesterases. J Biol Chem 1994, 269:30479–30484
12. Umezu-Goto M, Kishi Y, Taira A, Hama K, Dohmae N, Takio K, Yamori T, Mills GB, Inoue K, Aoki J, Arai H: Autotaxin has lysophospholipase D activity leading to tumor cell growth and motility by lysophosphatidic acid production. J Cell Biol 2002, 158:227–233
13. Clair T, Aoki J, Koh E, Bandle RW, Nam SW, Ptaszynska MM, Mills GB, Schiffmann E, Liotta LA, Stracke ML: Autotaxin hydrolyzes sphingosylphosphorylcholine to produce the regulator of migration, sphingosine-1-phosphate. Cancer Res 2003, 63:5446–5453
14. Tanaka M, Okudaira S, Kishi Y, Ohkawa R, Iseki S, Ota M, Noji S, Yatomi Y, Aoki J, Arai H: Autotaxin stabilizes blood vessels and is required for embryonic vasculature by producing lysophosphatidic acid. J Biol Chem 2006, 281:25822–25830
15. Fuss B, Baba H, Phan T, Tuohy VK, Macklin WB: Phosphodiesterase I, a novel adhesion molecule and/or cytokine involved in oligodendrocyte function. J Neurosci 1997, 17:9095–9103
16. Palmeri D, Zuo FR, Rosen SD, Hemmerich S: Differential gene expression profile of human tonsil high endothelial cells: implications for lymphocyte trafficking. J Leukoc Biol 2004, 75:910–927
17. Kanda H, Newton R, Klein R, Morita Y, Gunn MD, Rosen SD: Autotaxin, an ectoenzyme that produces lysophosphatidic acid, promotes the entry of lymphocytes into secondary lymphoid organs. Nat Immunol 2008, 9:415–423
18. Okabe M, Ikawa M, Kominami K, Nakanishi T, Nishimune Y: 'Green mice' as a source of ubiquitous green cells. FEBS Lett 1997, 407:313–319
19. Förster R, Schubel A, Breitfeld D, Kremmer E, Renner-Muller I, Wolf E, Lipp M: CCR7 coordinates the primary immune response by establishing functional microenvironments in secondary lymphoid organs. Cell 1999, 99:23–33
20. Fukui Y, Hashimoto O, Sanui T, Oono T, Koga H, Abe M, Inayoshi A, Noda M, Oike M, Shirai T, Sasazuki T: Haematopoietic cell-specific CDM family protein DOCK2 is essential for lymphocyte migration. Nature 2001, 412:826–831
21. Akira S, Takeda K: Toll-like receptor signalling. Nat Rev Immunol 2004, 4:499–511
22. Ebisuno Y, Tanaka T, Kanemitsu N, Kanda H, Yamaguchi K, Kaisho T, Akira S, Miyasaka M: Cutting edge: the B cell chemokine CXC chemokine ligand 13/B lymphocyte chemoattractant is expressed in the high endothelial venules of lymph nodes and Peyer's patches and affects B cell trafficking across high endothelial venules. J Immunol 2003, 171:1642–1646
23. Nakano H, Tamura T, Yoshimoto T, Yagita H, Miyasaka M, Butcher EC, Nariuchi H, Kakiuchi T, Matsuzawa A: Genetic defect in T lymphocyte-specific homing into peripheral lymph nodes. Eur J Immunol 1997, 27:215–221
24. Izawa D, Tanaka T, Saito K, Ogihara H, Usui T, Kawamoto S, Matsubara K, Okubo K, Miyasaka M: Expression profile of active genes in mouse lymph node high endothelial cells. Int Immunol 1999, 11:1989–1998
25. Tatsuta T, Naito M, Oh-hara T, Sugawara I, Tsuruo T: Functional involvement of P-glycoprotein in blood-brain barrier. J Biol Chem 1992, 267:20383–20391
26. Niwa H, Yamamura K, Miyazaki J: Efficient selection for high-expression transfectants with a novel eukaryotic vector. Gene 1991, 108:193–199
27. Streeter PR, Rouse BT, Butcher EC: Immunohistologic and functional characterization of a vascular addressin involved in lymphocyte homing into peripheral lymph nodes. J Cell Biol 1988, 107:1853–1862
28. Streeter PR, Berg EL, Rouse BT, Bargatze RF, Butcher EC: A tissue-specific endothelial cell molecule involved in lymphocyte homing. Nature 1988, 331:41–46
29. Umemoto E, Tanaka T, Kanda H, Jin S, Tohya K, Otani K, Matsutani T, Matsumoto M, Ebisuno Y, Jang MH, Fukuda M, Hirata T, Miyasaka M: Nepmucin, a novel HEV sialomucin, mediates L-selectin-dependent lymphocyte rolling and promotes lymphocyte adhesion under flow. J Exp Med 2006, 203:1603–1614
30. Radeke HH, von Wenckstern H, Stoidtner K, Sauer B, Hammer S, Kleuser B: Overlapping signaling pathways of sphingosine 1-phosphate and TGF-β in the murine Langerhans cell line XS52. J Immunol 2005, 174:2778–2786
31. Toyama-Sorimachi N, Miyake K, Miyasaka M: Activation of CD44 induces ICAM-1/LFA-1-independent. Ca^{2+}, $Mg^{(2+)}$-independent adhesion pathway in lymphocyte-endothelial cell interaction. Eur J Immunol 1993, 23:439–446
32. Imamura S, Horiuti Y: Enzymatic determination of phospholipase D activity with choline oxidase. J Biochem (Tokyo) 1978, 83:677–680
33. Saito K, Tanaka T, Kanda H, Ebisuno Y, Izawa D, Kawamoto S, Okubo K, Miyasaka M: Gene expression profiling of mucosal addressin cell adhesion molecule-1^+ high endothelial venule cells (HEV) and identification of a leucine-rich HEV glycoprotein as a HEV marker. J Immunol 2002, 168:1050–1059
34. Mebius RE, Streeter PR, Michie S, Butcher EC, Weissman IL: A developmental switch in lymphocyte homing receptor and endothelial vascular addressin expression regulates lymphocyte homing and permits $CD4^+$ $CD3^-$ cells to colonize lymph nodes. Proc Natl Acad Sci USA 1996, 93:11019–11024
35. Michie SA, Streeter PR, Butcher EC, Rouse RV: L-selectin and α 4 β 7 integrin homing receptor pathways mediate peripheral lymphocyte traffic to AKR mouse hyperplastic thymus. Am J Pathol 1995, 147:412–421
36. Hiraoka N, Petryniak B, Nakayama J, Tsuboi S, Suzuki M, Yeh JC, Izawa D, Tanaka T, Miyasaka M, Lowe JB, Fukuda M: A novel, high endothelial venule-specific sulfotransferase expresses 6-sulfo sialyl $Lewis^{(x)}$, an L-selectin ligand displayed by CD34. Immunity 1999, 11:79–89
37. Hänninen A, Taylor C, Streeter PR, Stark LS, Sarte JM, Shizuru JA, Simell O, Michie SA: Vascular addressins are induced on islet vessels during insulitis in nonobese diabetic mice and are involved in lymphoid cell binding to islet endothelium. J Clin Invest 1993, 92:2509–2515
38. Boonstra A, Asselin-Paturel C, Gilliet M, Crain C, Trinchieri G, Liu YJ, O'Garra A: Flexibility of mouse classical and plasmacytoid-derived dendritic cells in directing T helper type 1 and 2 cell development: dependency on antigen dose and differential toll-like receptor ligation. J Exp Med 2003, 197:101–109
39. Tokumura A, Majima E, Kariya Y, Tominaga K, Kogure K, Yasuda K, Fukuzawa K: Identification of human plasma lysophospholipase D, a lysophosphatidic acid-producing enzyme, as autotaxin, a multifunctional phosphodiesterase. J Biol Chem 2002, 277:39436–39442
40. van Meeteren LA, Ruurs P, Stortelers C, Bouwman P, van Rooijen MA, Pradere JP, Pettit TR, Wakelam MJ, Saulnier-Blache JS, Mummery CL, Moolenaar WH, Jonkers J: Autotaxin, a secreted lysophospholipase D, is essential for blood vessel formation during development. Mol Cell Biol 2006, 26:5015–5022
41. Ohta H, Sato K, Murata N, Damirin A, Malchinkhuu E, Kon J, Kimura T, Tobo M, Yamazaki Y, Watanabe T, Yagi M, Sato M, Suzuki R, Murooka H, Sakai T, Nishitoba T, Im DS, Nochi H, Tamoto K, Tomura H, Okajima F: Ki16425, a subtype-selective antagonist for EDG-family lysophosphatidic acid receptors. Mol Pharmacol 2003, 64:994–1005
42. Jansen S, Callewaert N, Dewerte I, Andries M, Ceulemans H, Bollen M: An essential oligomannosidic glycan chain in the catalytic domain of autotaxin, a secreted lysophospholipase-D. J Biol Chem 2007, 282:11084–11091